Original Article

MOLECULAR METABOLISM

# Adipocyte lipid synthesis coupled to neuronal control of thermogenic programming

Adilson Guilherme [1,5], David J. Pedersen [1,5], Elizabeth Henchey [1], Felipe S. Henriques [1], Laura V. Danai [1,6], Yuefei Shen [1], Batuhan Yenilmez [1], DaeYoung Jung [1,2], Jason K. Kim [1,2], Irfan J. Lodhi [3], Clay F. Semenkovich [3,4], Michael P. Czech [1,*]

## ABSTRACT

**Background:** The de novo biosynthesis of fatty acids (DNL) through fatty acid synthase (FASN) in adipocytes is exquisitely regulated by nutrients, hormones, fasting, and obesity in mice and humans. However, the functions of DNL in adipocyte biology and in the regulation of systemic glucose homeostasis are not fully understood.

**Methods & results:** Here we show adipocyte DNL controls crosstalk to localized sympathetic neurons that mediate expansion of beige/brite adipocytes within inguinal white adipose tissue (iWAT). Induced deletion of FASN in white and brown adipocytes of mature mice (iAdFASNKO mice) enhanced glucose tolerance, UCP1 expression, and cAMP signaling in iWAT. Consistent with induction of adipose sympathetic nerve activity, iAdFASNKO mice displayed markedly increased neuronal tyrosine hydroxylase (TH) and neuropeptide Y (NPY) content in iWAT. In contrast, brown adipose tissue (BAT) of iAdFASNKO mice showed no increase in TH or NPY, nor did FASN deletion selectively in brown adipocytes (UCP1-FASNKO mice) cause these effects in iWAT.

**Conclusions:** These results demonstrate that downregulation of fatty acid synthesis via FASN depletion in white adipocytes of mature mice can stimulate neuronal signaling to control thermogenic programming in iWAT.



**Keywords** Adipocytes; de novo lipogenesis; iWAT browning; Glucose homeostasis; Sympathetic nerve activation

## 1. INTRODUCTION

Adipose tissue metabolism plays a paramount role in regulating energy balance and metabolic homeostasis, and its disruption is thus closely associated with metabolic diseases, such as obesity and diabetes [1–5]. Several studies have demonstrated major beneficial effects of implantation of adipocytes or adipose tissues derived from insulin sensitive mice into obese animals [5–8]. Three predominant pathways have been suggested whereby adipose tissue exerts such control over whole body glucose homeostasis. One hypothesis proposes a key role for sequestering triglyceride (TG) within adipocytes, reducing systemic "lipotoxicity" by keeping lipids away from disrupting sensitive pathways in other tissues such as liver and muscle [3,9]. A second concept focuses on extensive evidence that adipocytes display endocrine functions that play a pivotal role in controlling whole body metabolism [1,2,10,11]. Subsequent to the discoveries of the secreted adipose proteins leptin [12,13] and adiponectin [14], many other adipocyte-derived peptides that may modulate multiple organs (e.g., liver, brain, pancreas, skeletal muscle, and heart) important for the maintenance of energy balance and prevention of metabolic dysfunction have been identified [2,10,15–17]. A third concept of how adipose tissue might regulate systemic metabolic homeostasis invokes relatively new findings that brown adipose tissue (BAT) and "beige/brite" adipocytes within mouse and human white adipose tissues (WAT) might be major sites of fatty acid oxidation and energy expenditure [4,8,18]. These three concepts are not mutually exclusive, and, together, these pathways may operate synergistically to optimize adipose tissue depot influence on overall metabolic flux in mammals.

Initial work on adipocyte metabolism in obesity revealed that the biosynthesis of palmitate from acetyl CoA, denoted de novo lipogenesis (DNL), was markedly reduced in the insulin resistant state [19,20] in spite of near normal glucose uptake [21]. These data suggested a possible role of DNL disruption in insulin resistance of adipocytes that was extended to human adipose tissue [22,23]. These findings were initially puzzling, because DNL contributes only a few percent of fatty acids to the TG that accumulates in the lipid droplets of adipocytes [24–26]. More recently, however, a number of adipose-derived putative bioactive lipids that arise from DNL [27,28] have been identified,

[1]Program in Molecular Medicine, University of Massachusetts Medical School, Worcester, MA 01605, USA [2]Division of Endocrinology, Metabolism, and Diabetes, Department of Medicine, University of Massachusetts Medical School, Worcester, MA 01605, USA [3]Division of Endocrinology, Metabolism and Lipid Research, Washington University School of Medicine, St. Louis, MO 63110, USA [4]Department of Cell Biology and Physiology, Washington University School of Medicine, St. Louis, MO 63110, USA

[5] These authors contributed equally to this work.
[6] Current address: Koch Institute for Integrative Cancer Research and Department of Biology, Massachusetts Institute of Technology, Cambridge, MA 02139, USA.

*Corresponding author. Program in Molecular Medicine, University of Massachusetts Medical School, 373 Plantation Street, BIOTECH 2, Suite 100, Worcester, MA 01605, USA. Fax: +1 508 856 1617. E-mail: michael.czech@umassmed.edu (M.P. Czech).

Received April 17, 2017 • Revision received May 15, 2017 • Accepted May 25, 2017 • Available online 31 May 2017

http://dx.doi.org/10.1016/j.molmet.2017.05.012

  

including palmitoleate [29], the novel fatty acid—hydroxy—fatty acid (FAHFAs) lipids [30], and the recently identified PPARγ ligand alkyl ether-lipid (1-*O*-octadecenyl-2-palmitoyl-3-glycerophosphocholine) [31]. Beside biosynthesis of fatty acids, the DNL pathway is a rich source of metabolites known to regulate cellular processes, ranging from gene transcription to protein post-translational modifications (e.g., protein acetylation and palmitoylation) [32—36]. Nonetheless, experimental genetic manipulation of this pathway in adipocytes has produced conflicting results in terms of systemic effects [29,31,37,38], and the role of adipocyte DNL in both adipose function and systemic metabolic regulation remains unclear.

The aim of the present studies was to clarify the physiological role of adipocyte DNL by generating mouse models in which adipocyte FASN could be depleted after the animals reach maturity, thereby eliminating possible confounding effects of FASN knockout during mouse development. To this end, we generated a tamoxifen (TAM)-inducible adipose-specific FASN knockout mouse line (iAdFASNKO) in which FASN deletion and inhibition of DNL in adipocytes is initiated in adult mice. Analysis of these mice following FASN deletion revealed improved glucose tolerance and showed strong iWAT browning, with enhanced UCP1 and thermogenic gene expression, as previously found in constitutive adipocyte FASN knockout mice [31]. Surprisingly, however, depletion of FASN in primary white adipocytes in vitro failed to modulate UCP1 or other genes that are characteristically expressed at high levels in BAT, indicating that a cell autonomous mechanism is not involved and that an intact animal is required for the browning effect. This interpretation proved correct, as a markedly increased sympathetic innervation of iWAT was observed in response to induced FASN depletion in adipocytes of mature mice.

## 2. MATERIALS AND METHODS

### 2.1. Animal studies

Four-week old male C57BL/6J (WT) and B6.V-Lepob/J (ob/ob) mice were obtained from Jackson Laboratory. Mice were housed on a 12 h light/dark schedule and had free access to water and food, except when indicated. WT mice were fed a high fat diet (HFD) that contained 60% calories from lipids (Research Diets, D12492). Mice with conditional $FASN^{flox/flox}$ alleles were generated as described elsewhere [31]. To inactivate FASN in adult mice, homozygous $FASN^{flox/flox}$ animals were crossed to Adiponectin-Cre-ERT2 mice (a generous gift from Dr. Evan Rosen). At eight-weeks of age, both $FASN^{flox/flox}$ and $FASN^{flox/flox}$-Adiponectin-Cre-ERT2 (iAdFASNKO) were then treated once a day via intraperitoneal (i.p.) injection with 1—2 mg TAM dissolved in corn oil for 6 consecutive days. $FASN^{flox/flox}$ animals were also crossed with UCP1-Cre mice (Jackson Laboratory stock number 024670) to generate the UCP1-FASNKO that specifically delete FASN in brown adipocytes. For deletion of FASN in cultured primary adipocytes, $FASN^{flox/flox}$ mice were crossed with the TAM-inducible UBC-Cre-ERT2 mice (B6.Cg-Tg(UBC-cre/ERT2)1Ejb/2J mice, stock number 008085) from Jackson Laboratories.

All of the studies performed were approved by the Institutional Animal Care and Use Committee (IACUC) of the University of Massachusetts Medical School.

### 2.2. Metabolic studies

Glucose and insulin tolerance tests were performed on WT, iAdFASNKO, or UCP1-FASNKO mice as indicated. Glucose (1 g/kg) was administrated by i.p. injection. Blood samples were drawn from the tail vein at the indicated times, and glycemia was determined using a Breeze 2 glucose meter (Bayer and alpha-trak). For the effect of FASN deficiency on glucose tolerance, mice were first fed with chow or HFD for 4 weeks and then injected with vehicle or TAM to induce FASN deletion. Plasma insulin levels were measured with Millipore insulin ELISA.

### 2.3. Lipogenesis assay

To assess lipogenesis in vivo, hyperinsulinemic-euglycemic clamps were performed following an overnight fast, a 2-h hyperinsulinemic (insulin at 150 mU kg−1 body weight priming followed by 2.5 mU kg−1 min−1)-euglycemic clamp was conducted in awake mice using [$^{14}$C]-U-glucose to assess glucose metabolism in adipose tissue depots as described previously [39]. Tissues were then harvested, total neutral lipids extracted, and incorporation of glucose into TG or fatty acids determined as previously described [40]. For lipogenesis ex vivo, adipose tissue explants were incubated with labeling media containing 2% FA-free BSA, 1% (v/v) Pen/Strep, 0.5 mM D-Glucose, 0.5 mM Sodium Acetate, 2 mM sodium pyruvate, 2 mM glutamine, 2 μCi/mL $^{14}$C-U-glucose. Insulin at 1 μM was added to insulin-stimulated conditions. Adipose tissue explants were incubated at 37 °C in a humidified incubator (5% CO2) for 4.5 h before lipid extraction. Glucose incorporation into TG or into fatty acids was then determined as previously described [40]. To determine lipogenesis in cultured primary adipocytes, cells were incubated with labeling media with or without insulin for 4.5 h and total neutral lipid extracted as described.

### 2.4. Westerns blots

For in vivo insulin stimulated Akt phosphorylation, mice were fasted for 4 h, injected with phosphate-buffered saline (PBS) or insulin (1 IU/kg), and 15 min after the injection, tissues were harvested. For protein expression analyses, tissues were homogenized in lysis buffer (20 mM HEPES [pH 7.4], 150 mM NaCl, 2 mM EDTA, 1% Triton X-100, 0.1% SDS, 10% glycerol, 0.5% sodium deoxycholate) that had been supplemented with Halt protease and phosphatase inhibitors (Thermo Pierce). Samples from tissue lysates were then resolved by SDS-PAGE, and immunoblots were performed using standard protocols. Membranes were blotted with the following antibodies: AKT (S473 and total), ACLY, ACC, GAPDH, pHSL-S660, HSL, NPY, and perilipin (Cell Signaling Technology); FASN (BD Biosciences); UCP1 (Alpha Diagnostics); phospho-perilipin-S522 (Vala Sciences); TH (Abcam and Millipore), Tubulin (Sigma—Aldrich). Best results for western blotting of TH were obtained with Millipore-MAB318 antibody. For the ex vivo insulin signaling experiments, adipose tissue explants were incubated in Dulbecco's Modified Eagle Medium (DMEM) media supplemented with 0.5 mM glucose, 2 mM sodium pyruvate and 2 mM glutamine, in the absence or presence of 1 μM insulin for 30 min. Adipose tissue explants were then homogenized and total cell lysate immunoblotted with total and phospho-Akt.

### 2.5. Adipocyte isolation

For detection of FASN protein on isolated adipocytes, adipose tissues from control or iAdFASNKO were minced and digested, and the adipocytes were isolated as described previously [41].

### 2.6. Histological analysis

For the immunohistochemistry (IHC) and immunofluorescence (IF) of adipose tissue analyses, tissue samples were fixed in 4% paraformaldehyde and embedded in paraffin. Sectioned slides were then stained for H&E, UCP1 (Abcam) or for TH (Abcam) and DAPI, at UMASS Medical School Morphology Core. For immunofluorescence analyzes, photos from the stained adipose tissue sections were taken with an Axiovert 35 Zeiss microscopy (Zeiss, Germany) equipped with an Axiocam CCl camera at indicated magnification.

 

### 2.7. RNA isolation and RT-qPCR

Total RNA was isolated from cultured primary adipocytes or from mouse tissues using QIAzol Lysis Reagent Protocol (QIAGEN) following the manufacturer's instructions. cDNA was synthesized from 1 μg of total RNA using iScript cDNA Synthesis Kit (BioRad). Quantitative RT-PCR was performed using iQ SybrGreen supermix on BioRad CFX97and analyzed as previously described [42,43]. *36B4*, *Hprt*, *and Gapdh* served as controls for normalization. Primer sequences used for qRT—PCR analyses were listed in Supplementary Table 1.

### 2.8. Deletion of FASN in primary adipocyte cell culture

Primary white fat stromal vascular fraction (SVF) and mature fat cells from inducible-UBC-Cre-FASNKO mice were fractionated according to published methods [41]. Primary SVF cells were cultured in DMEM/F12 containing 10% FBS, 100 U $ml^{-1}$ penicillin, and 0.1 mg $ml^{-1}$ streptomycin (maintenance medium) until full confluence. Adipocyte differentiation was induced in preadipocyte cultures as previously described [44,45]. Briefly, confluent cells were treated for 48 h in maintenance medium containing 0.5 mM isobutylmethylxanthine, 60 μM indomethacin, 1 μM dexamethasone, 825 nM insulin and 1 μM rosiglitazone. Two days after induction, cells were switched to maintenance medium containing 825 nM insulin and 1 μM rosiglitazone. Then four days after induction, cells were switched to maintenance medium containing 825 nM insulin for 24 h, followed by maintenance medium only until harvested. For induction of FASN deletion in mature adipocytes, cells were treated with ethanol vehicle or with TAM (1 μM) for 24—48 h and medium replaced after this incubation time. Adipocytes were left for a further 48 h before further treatments or harvest. To determine $^{14}$C-glucose conversion into lipids, control and TAM-treated cells were starved for 2 h, incubated in labeling media with or without insulin for 4.5 h followed by lipid extraction. To examine the effect of FASN inhibition on DNL, control cells were preincubated for 1 h with 100 μM of FASN inhibitor platensimycin [46,47], followed by incubation with labeling media with or without insulin and lipid extractions after 4.5 h incubation. To stimulate *Ucp1* expression, cells were incubated with indicated CL316243 concentrations for 4 or 24 h, followed by total protein or RNA extractions for immunoblots or qPCR quantifications.

### 2.9. Statistical analysis

Data were analyzed in GraphPad Prism 7 (GraphPad Software, Inc.). The statistical significance of the differences in the means of experimental groups was determined by Student's *t*-test or one-way or two-way ANOVA and Fisher LSD posttests, as indicated. The data are presented as means ± SE. P values $\leq$ 0.05 were considered significant.

## 3. RESULTS

### 3.1. Early onset obesity downregulates DNL but not Akt activation in mouse adipose tissue

To determine whether the suppression in adipose tissue DNL arises at an early stage of obesity and whether it correlates with worsening of systemic glucose homeostasis, we analyzed expression levels of DNL genes in adipose tissue from diet- and genetically-induced obese mouse models. Despite the absence of major differences in weight gain at 5 weeks compared to WT mice, ob/ob mice were already markedly glucose intolerant and hyperinsulinemic [40], indicating a systemic metabolic dysfunction in this mouse model at this very early age. The mRNA expression of several lipogenic transcription factors and enzymes including *Fasn*, *Acly*, and *Elovl6* was also already markedly suppressed in the subcutaneous, inguinal adipose depot (iWAT) in these 5 week old ob/ob mice compared to WT mice (Figure 1A). The expression levels of these lipogenesis-related genes were even further downregulated at 7 and 11 weeks of age. We confirmed by protein immunoblotting that the protein products of lipogenic genes in adipose tissue from ob/ob mice were also decreased (Figure 1B). The DNL enzymes ATP-citrate lyase (ACLY), acetyl-CoA-carboxylase (ACC) and fatty acid synthase (FASN) were all significantly decreased in abundance in iWAT from 5 week old ob/ob mice (Figure 1B and Supplementary Figure 1). By contrast, expression of these lipogenic enzymes was remarkably upregulated in the livers of such ob/ob mice.

Using [$^{14}$C]-glucose as tracer, the in vivo and ex vivo rates of TG and de novo fatty acid biosynthesis in adipose tissue from ob/ob mice were also measured (Figure 2). While the insulin-stimulated glucose incorporation into total TG (fatty acid plus glycerol) was not reduced and basal TG biosynthesis significantly increased in the adipose tissue of ob/ob mice, glucose conversion to triglyceride fatty acids (TG-fatty acids) was strongly reduced in the adipose tissue of 7 week old ob/ob mice (Figure 2A). This was confirmed by measuring the rate of glucose-derived [$^{14}$C]-labeled carbon incorporation into TG-fatty acids in adipose tissue explants (ex vivo) in 7 week old and 11 week old mice (Figure 2B). Therefore, these results are consistent with the conclusion that DNL activity is severely attenuated at early stages of genetic obesity in mice. They also suggest that ob/ob mice utilize most of their glucose to synthesize glycerol in TG instead of fatty acids in adipose cells.

Since adipose glucose metabolism and flux through the DNL pathway are known to be regulated by signaling through the protein kinase AKT, we asked whether the decreased DNL in ob/ob mice might be mediated by disrupted insulin-induced AKT activation. Surprisingly, insulin-induced AKT activation was not affected by genetic obesity under conditions where DNL was markedly attenuated (Figure 2C). Together, these results indicate that inhibition of adipose tissue DNL in young ob/ob mice occurs independent of insulin signaling to AKT. Interestingly, a significant enhancement of basal AKT phosphorylation was observed in livers from ob/ob mice at these same ages (Supplementary Figure 2).

We further examined the relationship between systemic glucose intolerance, reduction of DNL-related genes and AKT activation in adipose tissue from mice fed a high fat diet short-term (1—4 weeks). As shown in Figure 3A—C, HFD feeding to 8 week old mice very rapidly causes glucose intolerance and insulin resistance. Strikingly, no significant changes in insulin-stimulated AKT activation were detected in adipose tissue from 1 week fed HFD mice (Figure 3D—E). In contrast, 1 week of HFD feeding also caused major reductions (about 90%) of several lipogenic enzymes (such as ACLY, FASN, and ACC) and inhibited adipose DNL activity (Figure 3F—H). Altogether, the results depicted in Figures 1—3 suggest that the reduction of adipose DNL and the worsening of systemic glucose homeostasis in early onset obesity are strongly correlated (Figure 3I), while hepatic DNL is increased under these same conditions. Moreover, while rapid and sustained defects in adipose DNL and in systemic insulin sensitivity were noted, the ability of insulin to induce phosphorylation of AKT remained intact in adipose tissue after 1—4 weeks of the HFD, reinforcing the notion that resistance to the actions of insulin on adipose glucose metabolism can be promoted by pathways downstream of insulin signaling to AKT [48].

### 3.2. Inducible deletion of adipocyte FASN in mature HFD fed mice improves glucose tolerance

The strong correlation between adipose DNL inhibition and glucose intolerance in obese mice suggests potential causative actions of

 

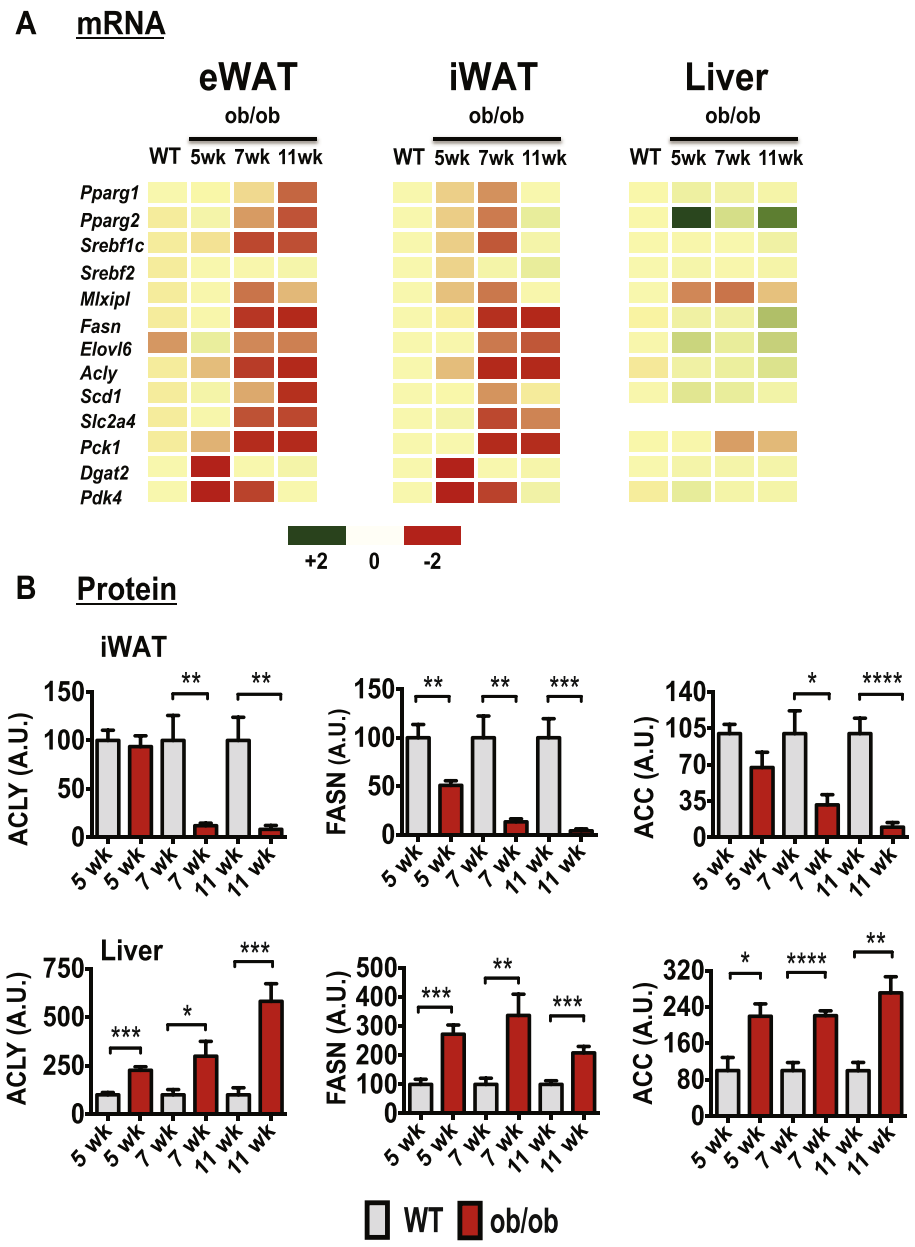


**Figure 1: Early onset obesity suppresses expression of genes encoding enzymes in the DNL pathway in adipose tissue, while enhancing expression of these genes in liver of ob/ob mice. (A):** Heat map representing the expression levels of genes involved in the DNL pathway. qPCR analyses were performed to determine relative gene expressions in epididymal (eWAT), inguinal subcutaneous (iWAT) fat tissues and livers from WT or littermate ob/ob mice at 5, 7, or 11 weeks of age; N = 4 - 5 mice per group. A green-red scale depicts normalized expression levels in fold-change compared to WT control mice. **(B):** Depicted are quantifications of ACLY, FASN, and ACC protein levels in iWAT or liver tissues from WT control or ob/ob mice at 5, 7, and 11 weeks of age. A.U., arbitrary units. N = 4–5 mice per group. Data are presented as mean −/+ SE and were compared to appropriate controls by Student's T-test. *P < 0.05; **P < 0.01; ***P < 0.001. ****P < 0.0001.

adipocyte DNL on systemic insulin sensitivity (Figure 3I). This notion is supported by a recent study reporting that constitutive adipose deletion of FASN improves glucose homeostasis in diet–induced obese mice [31]. To specifically test whether adipocyte DNL disruption after the onset of obesity in mice could affect systemic metabolic homeostasis, we developed an inducible adipocyte FASN KO mouse line in which deletion of adipocyte FASN can be initiated after the mice attain maturity. Thus, FASN floxed mice (with loxP flanked exons 4–8) [31] were crossed with a TAM-inducible adiponectin-Cre-ERT2 mouse line [49] to produce iAdFASNKO mice. TAM was administered via i.p. injections to both $FASN^{flox/flox}$ (control) and iAdFASNKO mice (Figure 4A), leading to a marked reduction of FASN in white and brown adipose tissue depots from iAdFASNKO mice, but not in liver, brain, or lung tissue, nor in any tissues in $FASN^{flox/flox}$ mice (Figure 4B–C). Moreover, isolation of adipocytes from TAM-treated iAdFASNKO mice followed by detection of FASN protein in cell lysates confirmed FASN reduction in adipocytes (Figure 4D).

We then investigated whether adipocyte deletion of FASN following diet-induced obesity could improve glucose tolerance. In these experiments, 8 week old mice were first fed HFD for 4 weeks to induce

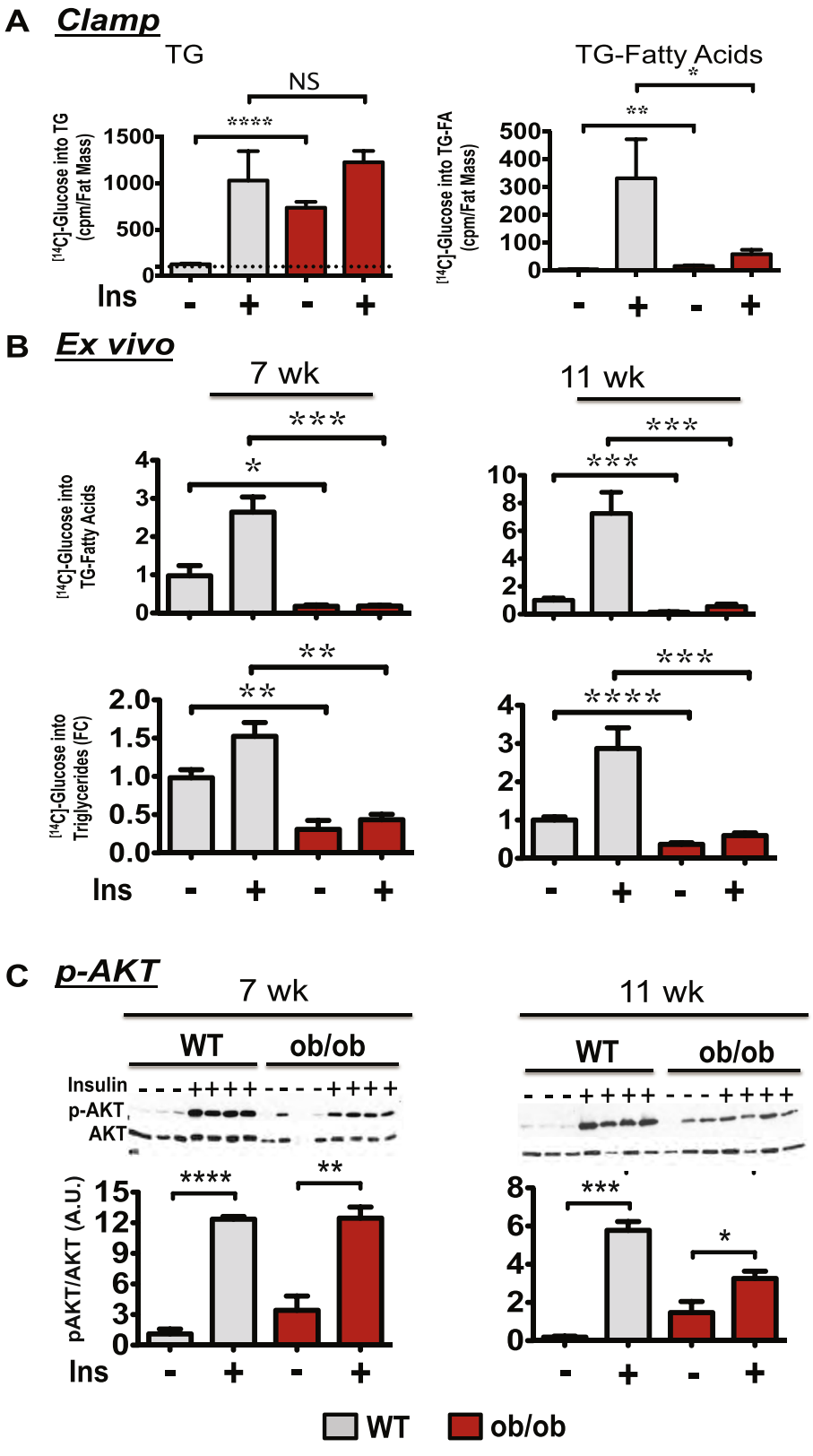


**Figure 2: Early onset obesity in ob/ob mice downregulates adipose tissue DNL, but not AKT activation. (A):** 7 week-old WT or ob/ob mice were fasted overnight and subjected to a 2 h hyperinsulinemic-euglycemic clamp with [$^{14}$C]-glucose to assess glucose conversion into lipids. Adipose tissues were then harvested and lipid extracted to determine glucose incorporation into TG or fatty acids. **(B):** Insulin-stimulated [$^{14}$C]-glucose conversion into TG and into TG-fatty acids were measured ex vivo in iWAT derived from 7 or 11 week old WT or ob/ob mice. **(C):** Representative protein immunoblot of AKT phosphorylation in iWAT in response to a bolus insulin injection (1 U/kg) as described in Materials and Methods. Bottom panels depict densitometry analysis of the data from the experiment described for top panel (N = 6 or 7). Graphs show the mean −/+ SEM. N = 5 to 7 per group, compared with WT controls, by Student's t test. *P < 0.05; **P < 0.01; ***P < 0.001; ****P < 0.0001.

 

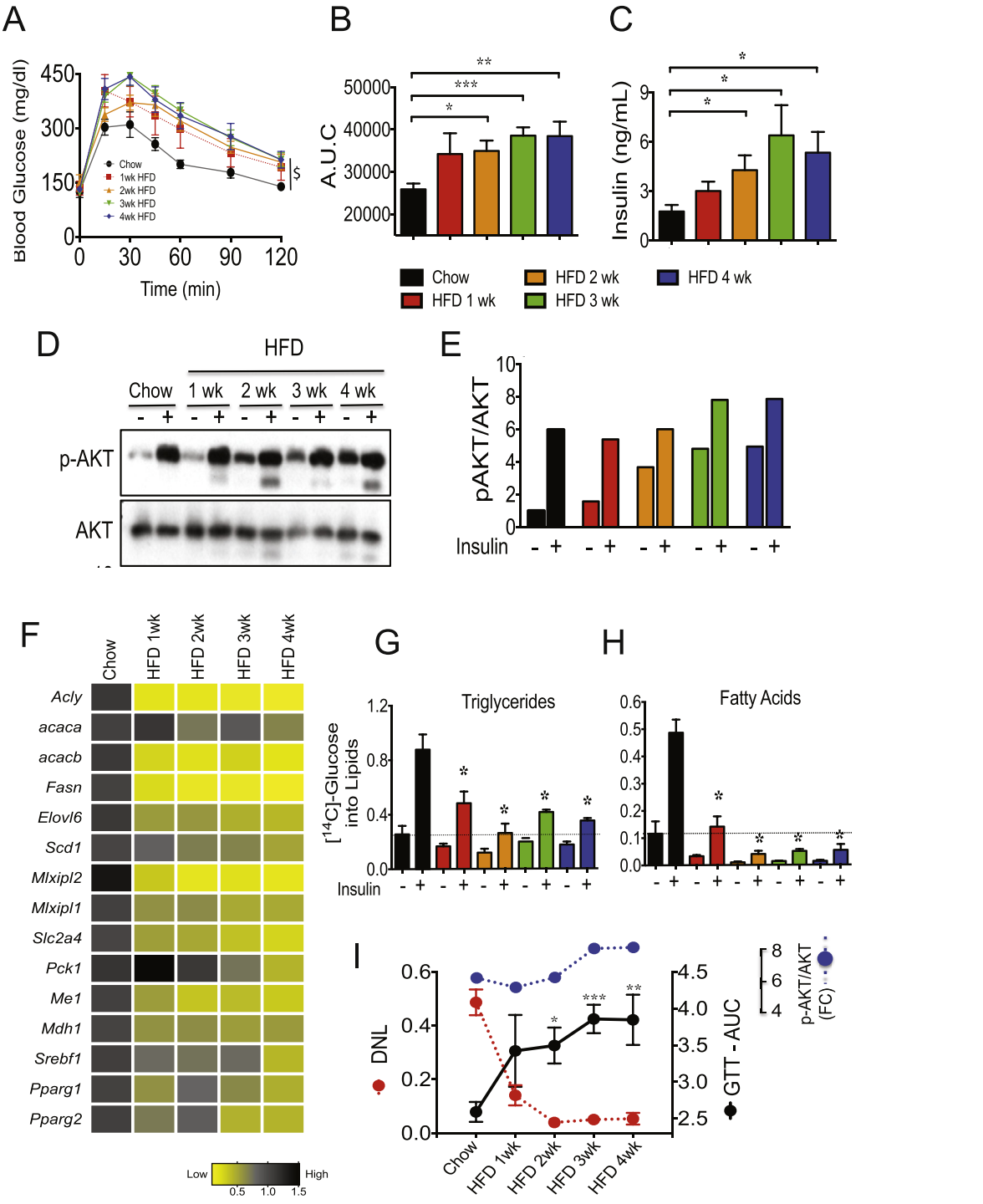


**Figure 3: Short-term HFD-feeding represses DNL but not AKT activation in adipose tissue. (A):** C57BL/6J male mice were fed for 1–4 weeks with chow or HFD and subjected to an oral GTT ($, $P < 0.0001$, two-way analysis of variance, $n = 5$). **(B):** Depicted is the area under the curve for the GTT. **(C)**: Plasma insulin levels in mice fed a chow or a HFD. **(D):** Short-term HFD feeding does not inhibit insulin-stimulated AKT activation in adipose tissue. iWAT explants from chow and HFD fed mice were stimulated with insulin in vitro for 30 min. Tissue lysates were then immunoblotted for total AKT and phospho-AKT (pAKT). **(E):** Quantification of p-AKT levels by densitometry analysis of data depicted in **D**. **(F):** HFD feeding strongly suppresses DNL genes in eWAT. Depicted is a heat map representing the expression levels of DNL genes in adipose tissues. qPCR analyses were performed to determine gene expression in eWAT from chow and HFD fed mice. $N = 5$ mice per group. A black-yellow scale depicts normalized expression levels in fold-change compared to chow fed controls mice. **(G, H)**: Insulin-stimulated [$^{14}$C]-glucose conversions into TG **(G)** and into TG-fatty acids **(H)** were measured in iWAT explants from chow and HFD fed mice. **(I):** Suppression of adipose tissue DNL by HFD feeding correlates with systemic glucose intolerance, while AKT activation is preserved. Depicted are the insulin-stimulated glucose conversions into fatty acids **(H)**, AKT activation **(E)** and the area under the curve (values multiplied by $10^{-3}$) for GTT **(B)** in 1–4 weeks HFD fed mice. Graphs show the mean −/+ SEM. $N = 5$ per group, compared with chow controls. Statistical significance was determined by Student's *t*-test or two-way ANOVA. *$P < 0.05$; **$P < 0.01$; ***$P < 0.001$.

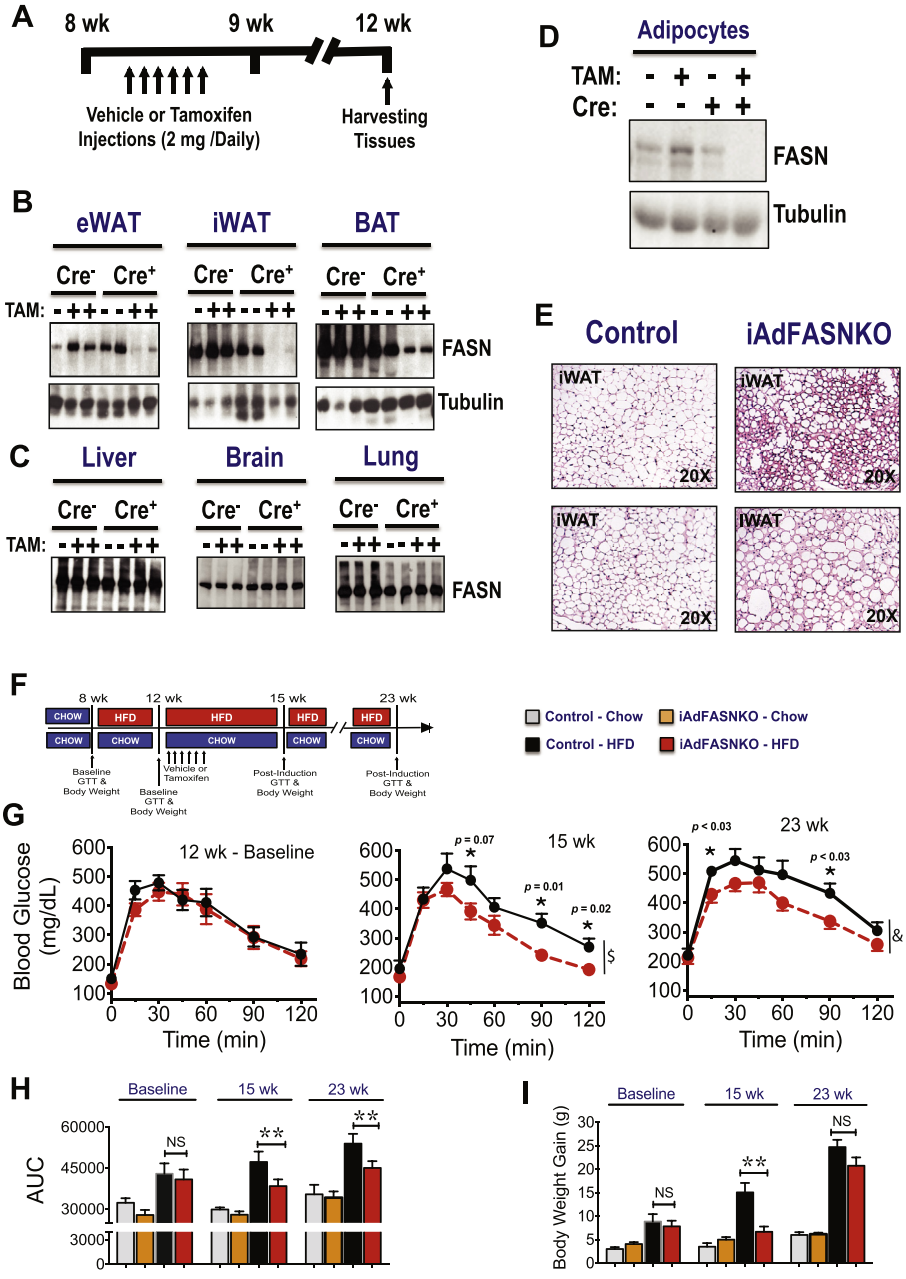


**Figure 4: Inducible deletion of adipocyte FASN in mature obese mice improves glucose tolerance. (A)**: Diagram representing the experimental design of TAM treatment to activate Cre-recombinase in adipose cells. 8-week-old mice were i.p. injected with 2 mg of TAM solubilized in sunflower oil or with sunflower oil only (vehicle control) for 6 days. Experiments were performed on littermate Cre-ERT2 -negative and Cre-ERT2 -positive mice 21 days after the last treatment of TAM. **(B, C):** TAM treatment induced deletion of FASN in adipose tissue from Cre-ERT2-positive mice but not in control mice. Epididymal (eWAT), subcutaneous (iWAT), brown fat (BAT), liver, and brain tissue lysates from Cre-ERT2-positive (Cre+), Cre-ERT2-negative (Cre-), vehicle, or TAM-treated (TAM) mice were immunoblotted for FASN or tubulin as indicated. **(D):** Isolated adipocytes from epididymal fat tissue from vehicle or TAM-treated mice were immunoblotted for FASN or tubulin as indicated. **(E)**: Histologic appearance of iWAT harvested from control or induced adipocyte FASN KO mice (iAdFASNKO). **(F):** Deletion of adipocyte FASN during HFD-feeding improves glucose tolerance. Diagram representing the experimental design. **(G):** Eight week old mice were HFD-fed for 4 weeks, and body weight gain and glucose tolerance measured before the TAM treatment (baseline measurements). At 3 and 13 weeks post-TAM treatment, glucose tolerance and body weight were measured again. Reductions in body weight gain **(I)** and attenuation of glucose intolerance **(G)** were observed in iAdFASNKO mice but not control mice. **(H)** The area under the curve for GTT is depicted. Statistical significance was determined by Student's *t*-test or two way ANOVA followed by Fisher LSD posttest. $, $P < 0.0001$, &, $P < 0.001$ two-way analysis of variance, $n = 4$ to 6 mice per group. *$P < 0.05$; **$P < 0.01$.

glucose intolerance (Figure 4F,G). Then the mice were treated with vehicle (controls) or with TAM to induce FASN deletion, and glucose tolerance tests (GTT) were performed 3 weeks and 11 weeks post-TAM treatment. As depicted in Figure 4G,H, FASN deletion in obese mice attenuated their glucose intolerance, and this beneficial effect persisted even 11 weeks after TAM induction. The metabolic improvement observed after FASN deletion is not due to changes in food intake (Supplementary Figure 3) and most likely not due to changes in body weight, as no differences in weight gain in iAdFANSKO mice were detected 11 weeks after deletion, despite persistent

 

improvement in glucose tolerance (Figure 4G,I). Thus, these results indicate that deletion of FASN in mature adipocytes after induction of obesity in mice ameliorates glucose intolerance, consistent with causative actions of adipocyte DNL on systemic metabolic homeostasis.

### 3.3. Inducible deletion of FASN in mature adipocytes enhances browning of iWAT without effect on BAT

Based on previous data indicating that constitutive inhibition of adipose DNL enhances browning in iWAT [31] and the increased multilocularity of lipid droplets in iWAT from iAdFASNKO mice revealed by

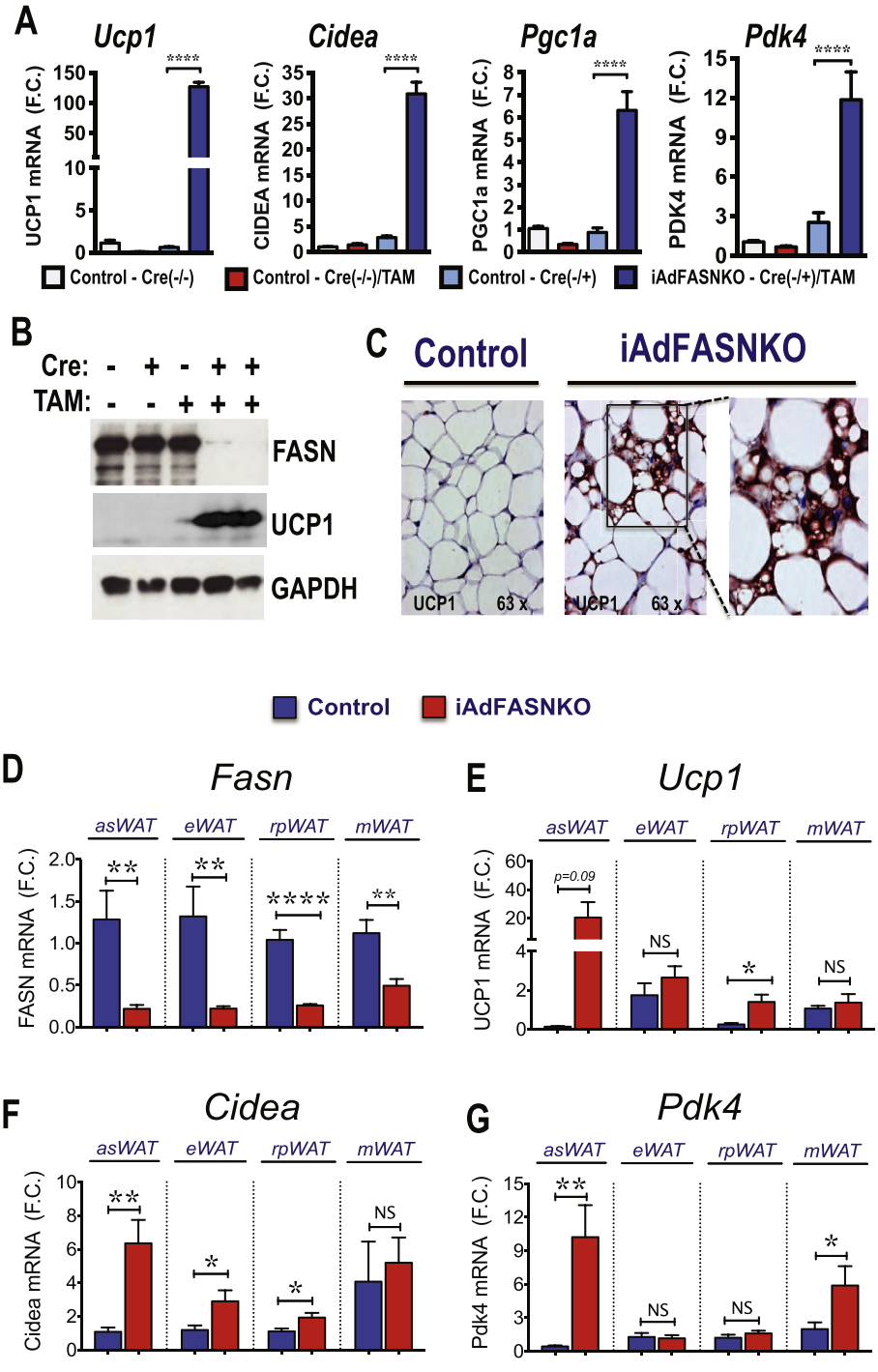


**Figure 5: Inducible deletion of adipocyte FASN in mature mice enhances browning of iWAT. (A):** qRT-PCR was performed for *Ucp1, Cidea, Pgc1a,* and *Pdk4* mRNA for quantifications in iWAT from indicated controls and iAdFASNKO (Cre+, TAM-treated) mice. N = 5–6 per group. **(B):** Inducible deletion of adipocyte FASN upregulates UCP1 protein in iWAT. iWAT lysates from controls and TAM-treated mice were immunoblotted for FASN, UCP1 or GAPDH as indicated. **(C):** Immunohistochemistry for UCP1 of iWAT from control or iAdFASNKO mice reveals UCP1 upregulation in the latter. Multilocular adipocytes are also detected in iAdFASNKO mice, but not control mice. Depicted are representative images of 5–7 mice per group. **(D–G)**: qPCR analysis to quantify mRNA expression levels of *Fasn, Ucp1, Cidea* and *Pdk4* in anterior subcutaneous (asWAT), epididymal (eWAT), retroperitoneal (rpWAT) and mesenteric (mWAT) adipose tissues from control or iAdFASN KO mice as indicated. N = 8 per group. *P < 0.05; **P < 0.01; ****P < 0.0001.

hematoxylin and eosin (H&E) staining (Figure 4E), we next examined whether inducible suppression of adipocyte FASN in mature mice also enhances thermogenic gene expression in WAT. As depicted in Figure 5A, TAM-induced FASN deletion in adipocytes induced strong upregulation of *Ucp1* mRNA along with increased expression of other characteristically expressed beige/brite/brown adipocyte genes, including cell death-inducing DNA fragmentation factor alpha-like effector A (*Cidea*), peroxisome proliferator-activated receptor a coactivator 1 (*Pgc1a*) and pyruvate dehydrogenase kinase isoform 4 (*Pdk4*) in iWAT. Immunoblot analysis confirmed that UCP1 protein level was also enhanced in iWAT from iAdFASNKO mice upon induction of FASN deletion by TAM (Figure 5B). Moreover, immunohistochemistry analysis revealed UCP1-positive multilocular adipocytes present in iWAT following TAM-induction of adipose-specific FASN knockout in mature mice, but not in control mice treated with TAM (Figure 5C).

The question of whether inducible adipose FASN deletion could enhance browning of other adipose depots was also addressed. As illustrated in Figure 5D, TAM treatment of iAdFASNKO mice efficiently reduced *Fasn* mRNA expression in anterior subcutaneous (asWAT), epididymal (eWAT), retroperitoneal (rpWAT), and mesenteric (mWAT) adipose tissue depots. Interestingly, while asWAT displayed upregulation of *Ucp1*, *Cidea*, and *Pdk4* mRNA expression upon FASN deletion, thermogenic gene expression in the other WAT depots was either only slightly enhanced (e.g., *Ucp1* and *Cidea* in rpWAT) or not affected by FASN deficiency (Figure 5E–G). Thus, the results depicted in Figures 4 and 6 indicate that along with enhanced systemic glucose tolerance, induced FASN depletion within adipocytes in mature mice potently induces browning of WAT primarily in subcutaneous fat depots.

The adiponectin-Cre mouse line used in our study induces deletion of FASN in both WAT and BAT, as illustrated in Figures 4B and 6A. We therefore examined whether white and brown adipocyte FASN deficiency affects the BAT thermogenesis program, like the effects observed in iWAT (Figure 5). Despite a strong suppression of FASN protein in BAT from TAM treated iAdFASNKO mice (Figure 6A), the expression of several thermogenesis-related genes in brown adipocytes, including *Ucp1, Cidea, Pgc1a*, and *Pdk4*, was not affected by FASN deletion (Figure 6C). Furthermore, no gross histological changes were detected in BAT following depletion of FASN, as assessed by (H&E) staining (Figure 6B). Thus, while induction of FASN deletion in white and brown adipocytes caused a marked upregulation of expression of thermogenesis-related genes and enhances browning in iWAT (Figure 5), BAT from mice under these same conditions did not appear to be affected by the absence of FASN enzyme in these experiments.

### 3.4. UCP1-cre driven FASN knockout in brown adipocytes does not improve glucose tolerance or browning of iWAT

To evaluate whether suppression of FASN in brown adipocytes could account for the iWAT browning and improved insulin sensitivity phenotype noted in the iAdFASNKO mice, $FASN^{flox/flox}$ animals were crossed to mice expressing a Cre-transgene driven by the UCP1-promoter to specifically delete FASN only in brown adipocytes (UCP1-FASNKO mice). $FASN^{flox/flox}$ littermates that do not express Cre-recombinase were used as controls. We confirmed specific deletion of FASN in BAT, but not in iWAT or eWAT adipose tissue depots in UCP1-FASNKO mice (Figure 7A). Additionally, FASN protein levels were preserved in liver, pancreas, and skeletal muscle from UCP1-FASNKO mice (Supplementary Figure 4A). However, as illustrated in Figure 7A, we found that deleting FASN only in BAT failed to elicit increases in UCP1 expression and browning of iWAT. Furthermore, deletion of FASN

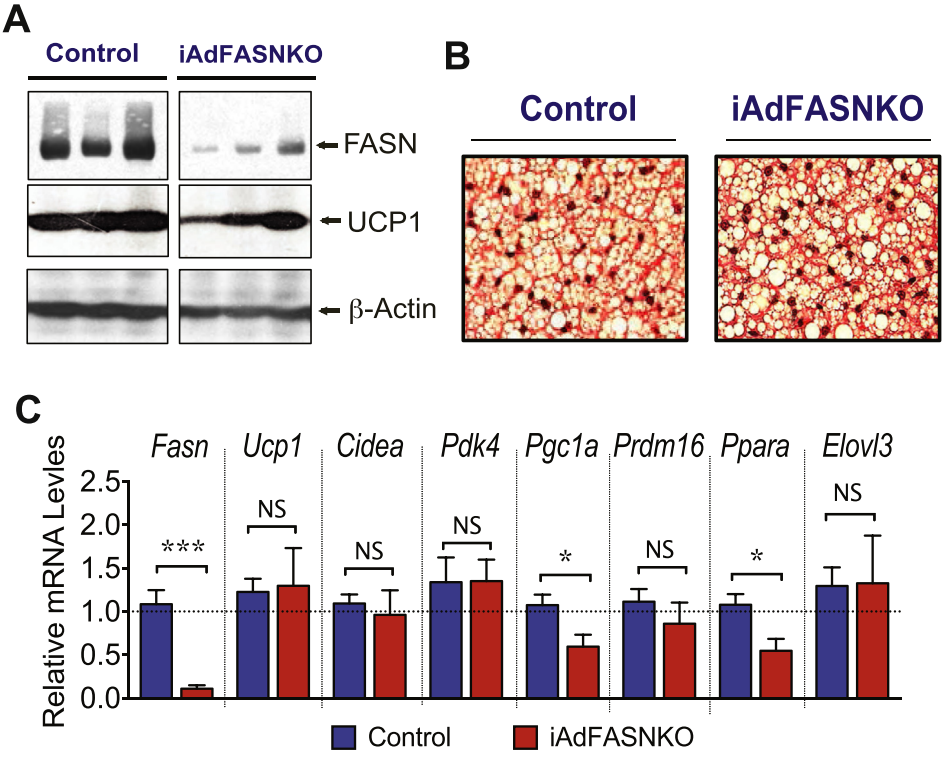


**Figure 6: Inducible adiponectin-Cre driven FASN deletion in adipocytes of mature mice does not enhance UCP1 expression and the thermogenic program in BAT. (A):** Inducible deletion of adipocyte FASN does not affect UCP1 protein in BAT. Tissue lysates from controls and iAdFASNKO mice were immunoblotted for FASN, UCP1, or actin as indicated. **(B):** H&E staining of BAT from control and iAdFASNKO mice reveals no major morphological changes in BAT upon FASN deletion. Depicted are representative images of 5–7 mice per group. **(C)**: qRT-PCR was performed for quantifications of indicated genes in BAT from controls and iAdFASNKO mice. N = 5–7 per group. *P < 0.05; ***P < 0.001.

 

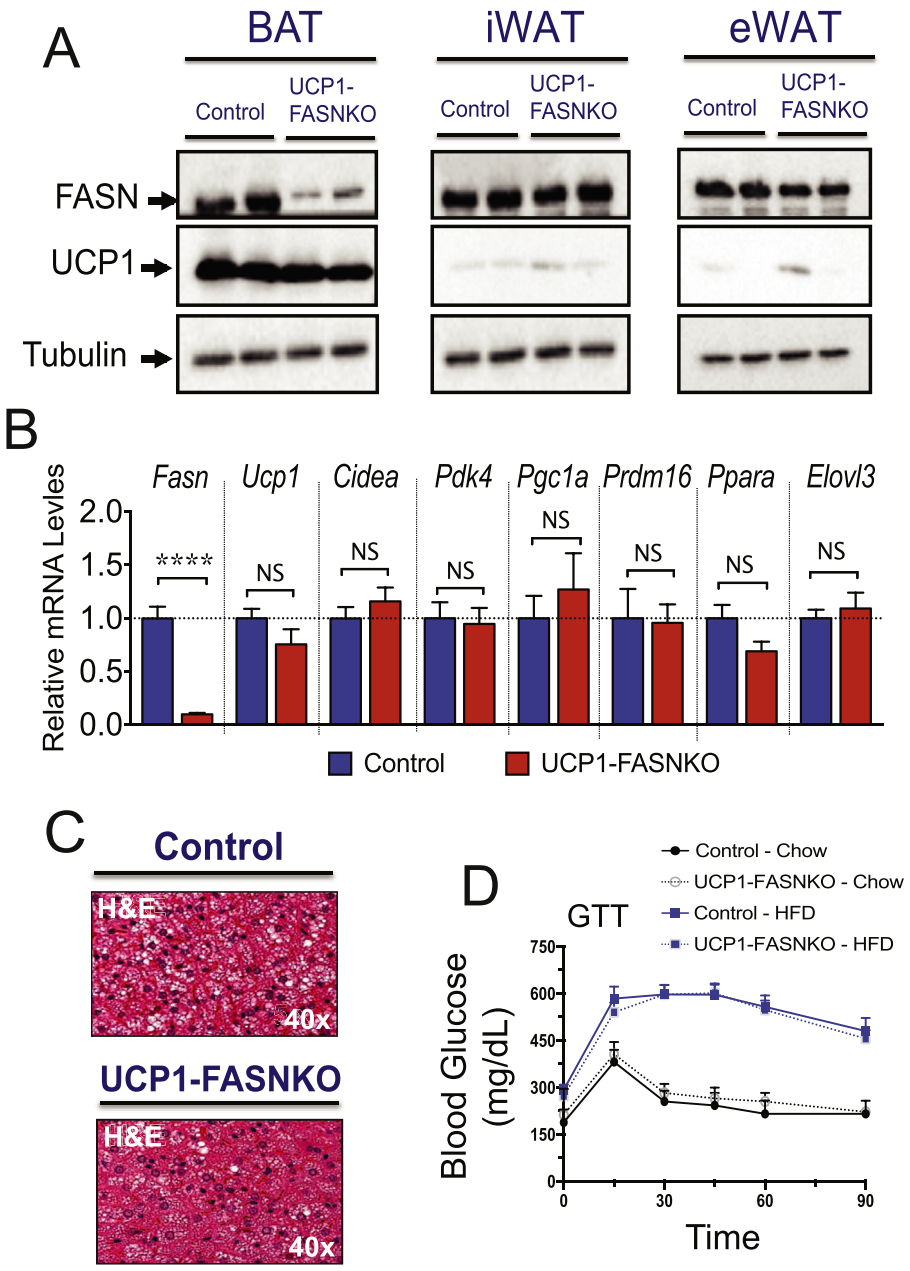


**Figure 7: UCP1-Cre driven FASN deletion in brown adipocytes of mature mice does not improve glucose tolerance or browning of iWAT. (A):** Adipose tissue lysates from control and UCP1-FASNKO mice were immunoblotted for FASN, UCP1, or tubulin protein as indicated. **(B):** qRT-PCR was performed for quantifications of indicated genes in BAT from controls and UCP1-FASNKO mice. N = 7–10. **(C):** H&E staining of BAT from control and UCP1-FASNKO mice. Depicted are representative images of 5–7 mice per group. **(D):** Diet-induced glucose intolerance is not ameliorated in UCP1-FASNKO mice. Control and UCP1-FASNKO mice were fed with chow or HFD for 12 weeks and then GTT performed. N = 3–6 mice per group. ****P < 0.0001.

in brown adipocytes did not affect the BAT thermogenic program, evidenced by lack of any detectable effects of FASN depletion on expression of thermogenesis-related genes (Figure 7B).

To assess whether brown adipocyte FASN ablation improves whole-body glucose metabolism in obese mice, control and UCP1-FASNKO mice were challenged with an HFD for 12 weeks. Control littermates and UCP1-FASNKO animals gained similar weight upon high-fat feeding, and body weights were unchanged between groups (Supplementary Figure 4B). Moreover, no alterations in GTT results were observed among control versus UCP1-FASNKO animals on chow or HFD (Figure 7D). Although BAT histology of UCP1-FASNKO mice revealed a slight decrease in brown adipocyte lipid droplet size compared to controls (Figure 7C), this modest alteration was not associated with significant changes in the BAT thermogenic program (Figure 7B). Thus, these results indicate that brown adipocyte FASN ablation does not enhance iWAT browning or improve insulin sensitivity in obese mice. The iWAT browning and increased glucose tolerance (Figures 4 and 5) in obese mice lacking FASN in both white and brown adipocytes thus appears to be due to depletion of FASN in white adipocytes.

### 3.5. Adipose FASN KO enhances sympathetic nerve outflow in iWAT

The inducible deletion of FASN in adipocytes depicted in Figures 4 and 5 indicates that reduced FASN expression in WAT can drive a program

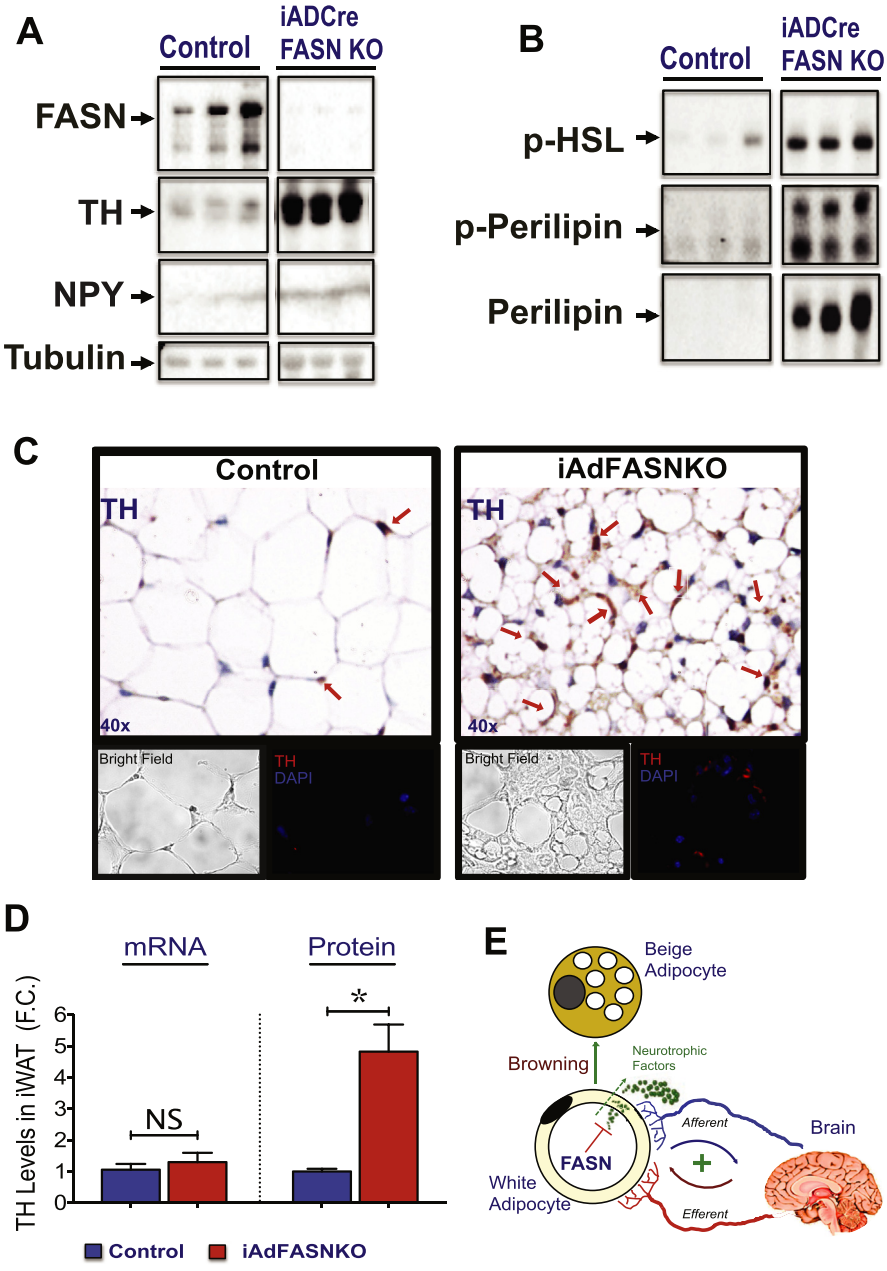


**Figure 8: Adipose FASN KO enhances sympathetic nerve outflow in iWAT. (A–B):** FASN deletion in adipocytes of mature mice increases tyrosine hydroxylase (TH) and neuropeptide Y (NPY) content and activates the PKA signaling pathway in iWAT. Depicted are representative immunoblots to detect FASN, TH, NPY, and tubulin **(A),** phospho-HSL, phospho-perilipin, and perilipin **(B)** levels in iWAT from control or iAdFASNKO mice. **(C):** Immunohistochemistry (top panels) and immunofluorescence (bottom panels) analysis for detection of TH content in iWAT from control and iAdFASNKO mice. **(D):** Quantification of *Th* mRNA and TH protein levels in iWAT upon induction of adipocyte FASN deletion. *Th* mRNA was quantified by qPCR and TH protein levels through densitometry from immunoblot data shown in A. N = 6–8 mice per group. *P < 0.05. **(E):** Proposed model shows how deletion of FASN in white adipocytes may enhance adipose browning through neuronal circuit regulation.

of adaptive thermogenesis in vivo. Based on extensive data [18,50–53] indicating that a major pathway of iWAT browning is through activation of the sympathetic nervous system (SNS), we evaluated whether adipocyte FASN KO elicits localized SNS activation to cause upregulation of UCP1 and expression of other browning genes in iWAT. To address this question, the effects of adipocyte FASN deletion on neuronal tyrosine hydroxylase (TH) and neuropeptide-Y (NPY) levels in iWAT were investigated. As shown in Figure 8A, a marked increase in both TH and NPY contents were detected in iWAT from iAdFASNKO mice. Moreover, these results were confirmed by immunohistochemistry and immunofluorescence of whole iWAT from mice deficient in FASN, which showed marked increases in staining intensity and in the number of locations of staining with anti-TH antibody (Figure 8C). In addition, cAMP signaling in iWAT was induced upon FASN KO, based on increases in phospho-perilipin, perilipin, and phospho-HSL levels (Figure 8B) and measurements of adipocyte cAMP itself (data not shown). Interestingly, the enhanced TH in iWAT depleted of FASN is reflected at the protein level, but not at the mRNA level (Figure 8D).

 

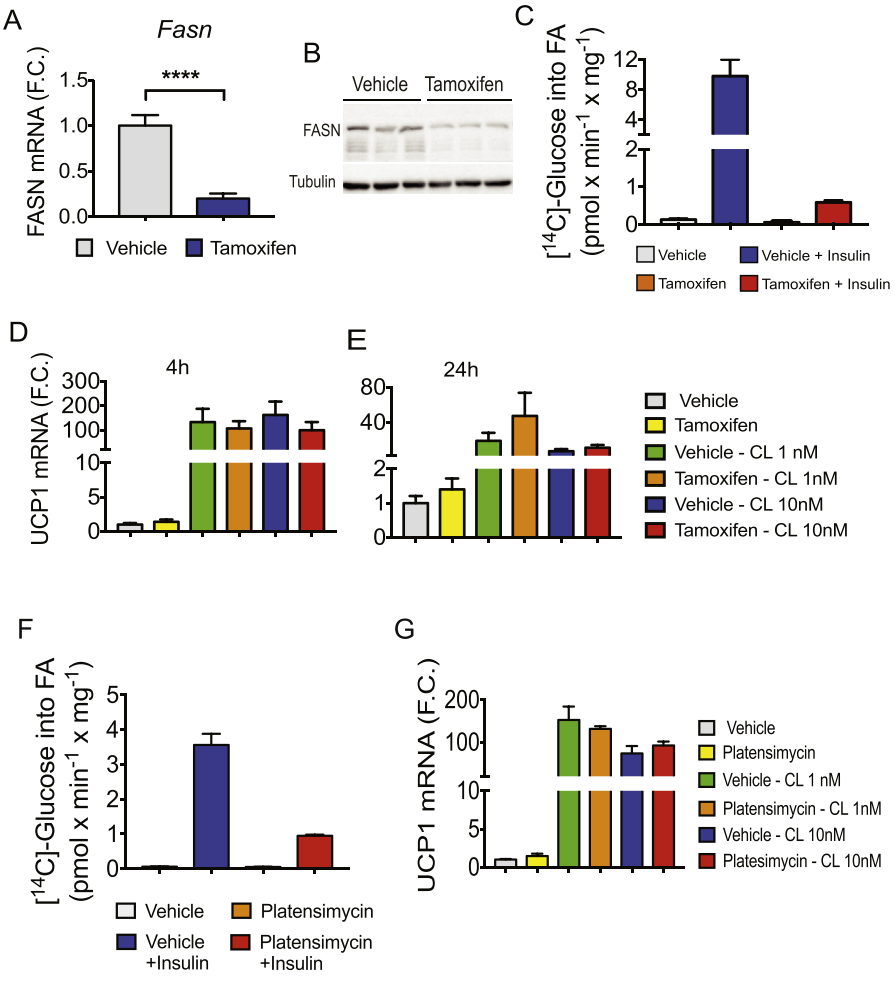


**Figure 9: Inhibition of DNL does not enhance thermogenic gene expression in cultured primary iWAT adipocytes in vitro. (A):** Subcutaneous preadipocytes in the SVF of inguinal fat from inducible-UBC-Cre-FASNKO mice were differentiated in vitro into mature adipocytes. The mature adipocytes were treated with vehicle or TAM to induce FASN deletion. Depicted in **(A)** is the qPCR quantification of *Fasn* mRNA in control or TAM-treated cells. **(B)** Immunoblots to detect FASN and tubulin protein expression levels in control and TAM-treated adipocytes. **(C):** Insulin-stimulated [$^{14}$C]-Glucose conversion into fatty acids in control or in FASN-deleted primary adipocytes. **(D–E)** mRNA levels of *Ucp1* in control and FASN KO adipocytes stimulated for 4 or 24 h with indicated doses of CL316243 were determined. **(F):** Primary adipocytes from WT mice were pretreated with 0.1 mM of FASN inhibitor platensimycin, then the insulin stimulation of [$^{14}$C]-Glucose into fatty acids determined. **(G):** mRNA levels of *Ucp1* in control and in platensimycin-pretreated adipocytes, stimulated for 4 h with indicated doses of CL316243, were determined. ****P $<$ 0.0001.

These data strongly indicate that the TH signals we detect are derived from neurites projecting into adipose tissue rather than from other cell types infiltrating the tissue. Altogether, these results are consistent with the hypothesis that adipocyte DNL activity is linked to control of local SNS activity.

The data in Figure 8 indicate that an intact animal may induce adipose browning in response to adipocyte FASN depletion and predict that cell autonomous effects of FASN deletion to enhance UCP1 expression may not operate under the conditions of our experiments. To address this question, primary preadipocytes of WAT from inducible-UBC-Cre-FASNKO mice were isolated and differentiated into adipocytes. The mature adipocytes were then treated with TAM or control conditions to induce FASN depletion, and the effect of FASN ablation on *Ucp1* mRNA expression in these cultured adipocytes in vitro was evaluated. As shown in Figure 9A,B, endogenous *Fasn* mRNA and protein levels were efficiently decreased by TAM treatment of the cells derived from inducible-UBC-Cre-FASNKO mice but not by vehicle control treatment. Moreover, loss of FASN from differentiated adipocytes caused a marked reduction in [$^{14}$C]-glucose conversion into fatty acids, confirming inhibition of the DNL pathway in adipocytes upon deletion of FASN (Figure 9C). To determine whether deletion of FASN increases thermogenesis-related gene expression cell autonomously, primary adipocytes depleted or not of FASN enzyme were treated for 4 or 24 h with indicated doses of the β3-adrenoreceptor agonist CL316243, followed by *Ucp1* mRNA quantification. As shown in Figure 9D,E, loss of FASN from differentiated adipocytes did not enhance *Ucp1* mRNA expression in either basal or CL316243-stimulated conditions.

To further investigate whether suppression of DNL affects UCP1 expression in vitro, we treated differentiated adipocytes with the potent FASN inhibitor platensimycin [46,47] then stimulated the cells with CL316243 and examined *Ucp1* expression. Despite the strong inhibition of [$^{14}$C]-glucose incorporation into fatty acids (Figure 9F), platensimycin treatment failed to enhance *Ucp1* expression in basal or CL-stimulated adipocytes (Figure 9G). Therefore, inhibition of DNL does not enhance thermogenic gene expression in cultured primary

 

adipocytes derived from WAT, suggesting that the enhanced browning in iWAT depleted from FASN (Figure 5) is not cell autonomous under our experimental conditions.

## 4. DISCUSSION

The major finding of these present studies indicates that disruption of adipocyte FASN, the final enzyme in the highly regulated DNL pathway (Figures 1–3), initiates neuronal signaling that triggers sympathetic stimulation of iWAT (Figure 8), activation of the cAMP pathway (Figure 8) and browning of this adipose depot (Figures 4 and 5). These effects are associated with marked upregulation of the expression of iWAT UCP1 and other genes characteristic of BAT (Figure 5), expansion of beige/brite cells with a multilocular phenotype in iWAT (Figure 5), and improved glucose tolerance (Figure 4). Enhanced iWAT sympathetic innervation upon adipocyte FASN depletion is supported by increased abundance of TH and NPY in this adipose depot and induction of cAMP signaling (Figure 8). That this is a major mechanism of iWAT browning in iAdFASNKO mice is further supported by the failure of isolated primary adipocytes to display UCP1 expression or other characteristics of beige/brite cells in vitro upon FASN depletion (Figure 9). Thus, intact mice manifest iWAT browning with adipocyte FASN knockout through a fully functional neuronal network. Taken together, these data demonstrate that DNL, a key pathway of lipid metabolism in adipocytes, may be coupled to modulation of adipose sympathetic tone, which in turn controls major adipose tissue functions including expansion of beige/brite cells. This pathway of adipocyte-neuron crosstalk may also have major implications for control of whole body metabolic homeostasis.

An important question raised by our results is whether the enhanced browning of iWAT in iAdFASNKO mice is secondary to effects initiated in BAT or WAT or both, since adipocytes in both depots are depleted of FASN in these mice. Compensatory mechanisms of WAT browning due to inhibition of BAT thermogenesis have been reported [18,54], for example, upon genetic ablation of the BMP receptor (*Bmpr1a*) in brown adipocyte progenitor cells [54]. This leads to a paucity of BAT, compensatory increased sympathetic input to WAT, and browning [54]. We addressed this possibility by examining thermogenesis in both BAT and WAT from iAdFASNKO mice as described above as well as from UCP1-FASNKO mice, which lack FASN only in brown adipocytes. Despite the efficient depletion of FASN protein in brown adipocytes from both mouse lines, no changes in thermogenic gene expression in BAT were detected (Figures 6 and 7), indicating that the FASN pathway in BAT does not regulate BAT thermogenesis under the experimental conditions used in our study. Notably, suppression of FASN in brown adipocytes also did not promote browning of WAT and failed to improve systemic insulin sensitivity in obese mice (Figure 7) as is the case for iAdFASNKO mice. These findings indicate that FASN deletion in WAT, not BAT, must be mediating the iWAT browning observed in iAdFASNKO mice (Figure 5). The strong implication of these findings is that adipocytes in WAT initiate neuronal signaling in a WAT tissue-dependent manner rather than through a compensatory mode in response to BAT dysfunction.

Previous studies have addressed the point that adipocyte DNL is a highly regulated pathway, as in fasting [55] and obesity [19,20,56,57], and it is generally correlated with the degree of systemic insulin sensitivity [27,28,37,40,56,57]. Our studies further confirm that suppression of the adipose DNL pathway and deterioration of systemic glucose metabolism are tightly correlated very early in obesity (Figures 1–3), even when Akt is fully sensitive to insulin (Figure 2). Several reports have suggested that adipocyte DNL activity is causative in mediating improved systemic glucose tolerance based on genetic manipulation of upstream components of the pathway to modulate production of putative insulin sensitizing lipids [29,37,38]. On the other hand, previous work on the constitutive deletion of adipocyte FASN led to the opposite conclusion [31]. These confounding results prompted us to use a more acute FASN deletion model that could be used in mature mice (iAdFASNKO mice), eliminating possible effects of FASN loss during early mouse development. Our results using this iAdFASNKO mouse model support the concept that FASN controls a pathway that normally suppresses iWAT browning and glucose tolerance, and that inhibition of DNL releases this suppression through activation of neuronal signaling and increased sympathetic activity. However, depletion of FASN does not exactly mimic the decreased DNL that occurs in obesity since other enzymes in the DNL pathway are also downregulated in HFD mice. Therefore, it is not yet clear how the results presented here relate to the body of literature suggesting that adipocyte DNL is actually beneficial to glucose homeostasis. Such clarification will likely require experiments designed to elucidate the molecular mechanisms through which adipocyte FASN depletion enhances adipose tissue TH levels.

There is a close anatomical and functional relationship between adipose tissue and SNS and the interplay between these two organs is vital to energy balance and metabolic homeostasis. On the one hand, BAT is highly innervated, with extensive sympathetic and sensory nerves that secrete factors to regulate lipolysis and thermogenesis [58], while WAT is less innervated [53] but does require neuronal secretion of catecholamines for stimulation of lipolysis during fasting [59]. Recent research shows that stimulation of cAMP is propagated in WAT through the action of the gap junction protein connexin 43, thus amplifying the effects of localized β adrenergic stimulation and increasing the browning of WAT [60]. Importantly, blocking SNS outflow in WAT through local denervation suppresses both cold-induced thermogenesis in BAT and browning in WAT, consistent with an essential role of SNS in adipose tissue physiology [51–53,60,61]. On the other hand, adipose-derived factors, such as leptin [62–65] and fatty acids from lipolysis, activate local sensory neurons in WAT to elicit thermoregulation in BAT [61]. Moreover, deletion of leptin signaling in sensory neurons results in obesity [64]. Altogether, these studies highlight the existence of an active inter-organ communication between adipose tissue and brain, indispensable to maintain energy and metabolic balances. Our findings add to the understanding of this crosstalk between adipose tissue and the nervous system, and pinpoint the metabolic pathway of DNL as a potential aspect of the mechanism whereby this crosstalk is mediated. Might signaling by the adipocyte DNL pathway to modulate adipose sympathetic tone be an important mechanism of regulation under physiological conditions? While direct data are not available, fasting and refeeding would seem to be good candidate physiological states for such control to occur. For example, the virtual complete blockade of adipocyte FASN activity during fasting, like the experimental FASN depletion shown here (Figure 4), would be a logical contributor to the enhancement of sympathetic activity in iWAT known to occur upon food restriction. Interestingly, DNL contributes very little to total fat deposition within the lipid droplets of adipocytes, which mostly derives from lipoprotein lipase (LPL)-mediated hydrolysis of circulating lipoproteins [24–26,66]. This suggests that DNL has other roles in the adipocyte. Its tight relationship with a variety of signaling molecules and key substrates for other major pathways, for example acetyl CoA as substrate for protein acetylations [33,34] and palmitate as substrate for protein palmitoylations [35,36], may be indicative of high impact regulatory roles, as exemplified by neuronal modulation shown here. A key question for future studies is what are the cell autonomous mechanisms triggered by FASN depletion that mediate activation of neuronal stimulation.

 

While the role of adipose tissue in regulation of whole body metabolism is now well established, less is known about the signaling mechanisms and pathways within adipocytes that control systemic homeostasis. Over the last two decades, however, the contribution of adipose-derived molecules to whole body glucose metabolism has been intensively investigated and a role for these molecules in systemic metabolism through activation of central nervous system (CNS) has been proposed [1,51,61–64]. For instance, adipose secretion of leptin exerts some of its systemic effects on metabolism partially through activation of sensory nerves in adipose tissue [64]. Also, free fatty acids derived from adipocyte lipolysis seem to function as mediators of adipocyte-neuron communications, as they appear to stimulate local sensory nerves in WAT eliciting thermogenesis in BAT [61]. Nonetheless, whether the adipose DNL pathway can produce signaling metabolites that control SNS innervation in WAT had not been demonstrated previously. Therefore, our study describes for the first time a potentially important link between the adipocyte DNL pathway and the SNS outflow to WAT. This connection appears to be functionally relevant, as inhibition of adipose DNL enhanced WAT innervation along with improved energy and systemic metabolic homeostasis in obese mice (Figures 4, 5, and 8). Altogether, these results are consistent with the hypothesis that metabolites or other factors derived from blockade of the adipocyte DNL pathway may control the activation of local afferent neurons. According to this model, upon deletion of adipocyte FASN and inhibition of DNL, these activated sensory neurons signal to the CNS to enhance SNS expansion and browning in iWAT (Figure 8E). However, our data do not rule out direct effects of FASN depletion on sympathetic fibers in adipose tissue. In any case, we hypothesize that the adipose DNL pathway may function as a fine-tuned control mechanism for SNS activation in WAT and may be essential for optimal energy balance and metabolic homeostasis.

Although inducible knockout mouse models are valuable tools to study post-developmental function of genes, one caveat is that some non-specific effects associated with TAM treatment, particularly on adipose cell differentiation, could make the use of TAM-inducible mouse lines less suitable for metabolic studies [67]. Nevertheless, the results described in our studies are clearly due to FASN deletion, as control Cre (−/−) mice treated with same doses of TAM did not display WAT browning or changes in glucose tolerance (Figures 4 and 5). Also, as expected, FASN protein levels in adipocytes from Cre (−/−) mice were not affected by the drug treatment (Figures 4–9).

## 5. CONCLUSIONS

In summary, the findings presented here suggest that suppression of FASN in white adipocytes from mature mice enhance sympathetic activity and induce browning in WAT and improve glucose homeostasis in obese mice. These data support the hypothesis that fatty acid biosynthesis in white adipocytes controls thermogenic programming in iWAT and systemic metabolic homeostasis through neuronal regulation. This hypothetical pathway may also be relevant to dysfunctions in systemic glucose tolerance that occur in obesity and diabetes [68]. A key question raised by these results relates to the molecular identity of the signal or signals arising from the adipocyte DNL pathway that activate neuronal signaling. Identification of such signals will be the focus of future experiments.

## AUTHOR CONTRIBUTIONS

A.G., D.J.P., L.V.D., and M.P.Czech designed research. A.G. and M.P.Czech wrote the manuscript. D.J.P. reviewed the manuscript. A.G., D.J.P., E.H., F.H., L.V.D., Y.S, B.Y., J.C.Y., and D.J. performed research. I.J.L and C.F.S designed the FASN-floxed mouse model that was used in the research. D.J and J.K.K. designed and performed the mouse metabolic clamp studies.

## ACKNOWLEDGMENTS

We thank all members of Michael Czech's Lab for helpful discussions and critical reading of the manuscript. We thank the UMASS Morphology Core for assistance. This work was supported by NIH grants DK30898 and DK103047 to M.P.C, and part of this study was performed at the National Mouse Metabolic Phenotyping Center at UMASS funded by NIH grant 2U2C-DK093000.

## CONFLICT OF INTEREST

The authors declare no conflict of interest.

## APPENDIX A. SUPPLEMENTARY DATA

Supplementary data related to this article can be found at http://dx.doi.org/10.1016/j.molmet.2017.05.012.

## REFERENCES

[1] Stern, J.H., Rutkowski, J.M., Scherer, P.E., 2016. Adiponectin, leptin, and fatty acids in the maintenance of metabolic homeostasis through adipose tissue crosstalk. Cell Metabolism 23(5):770–784.

[2] Kusminski, C.M., Bickel, P.E., Scherer, P.E., 2016. Targeting adipose tissue in the treatment of obesity-associated diabetes. Nature Reviews Drug Discovery 15(9):639–660.

[3] Guilherme, A., Virbasius, J.V., Puri, V., Czech, M.P., 2008. Adipocyte dysfunctions linking obesity to insulin resistance and type 2 diabetes. Nature Reviews Molecular Cell Biology 9(5):367–377.

[4] Rosen, E.D., Spiegelman, B.M., 2014. What we talk about when we talk about fat. Cell 156(1–2):20–44.

[5] Tran, T.T., Kahn, C.R., 2010. Transplantation of adipose tissue and stem cells: role in metabolism and disease. Nature Reviews Endocrinology 6(4):195–213.

[6] Konrad, D., Rudich, A., Schoenle, E.J., 2007. Improved glucose tolerance in mice receiving intraperitoneal transplantation of normal fat tissue. Diabetologia 50(4):833–839.

[7] Hocking, S.L., Chisholm, D.J., James, D.E., 2008. Studies of regional adipose transplantation reveal a unique and beneficial interaction between subcutaneous adipose tissue and the intra-abdominal compartment. Diabetologia 51(5):900–902.

[8] Min, S.Y., Kady, J., Nam, M., Rojas-Rodriguez, R., Berkenwald, A., Kim, J.H., et al., 2016. Human 'brite/beige' adipocytes develop from capillary networks, and their implantation improves metabolic homeostasis in mice. Nature Medicine 22(3):312–318.

[9] Czech, M.P., Tencerova, M., Pedersen, D.J., Aouadi, M., 2013. Insulin signalling mechanisms for triacylglycerol storage. Diabetologia 56(5):949–964.

[10] Luo, L., Liu, M., 2016. Adipose tissue in control of metabolism. Journal of Endocrinology 231(3):R77–R99.

[11] Kwon, H., Pessin, J.E., 2013. Adipokines mediate inflammation and insulin resistance. Frontiers Endocrinology (Lausanne) 4:71.

[12] Zhang, Y., Proenca, R., Maffei, M., Barone, M., Leopold, L., Friedman, J.M., 1994. Positional cloning of the mouse obese gene and its human homologue. Nature 372(6505):425–432.

[13] Halaas, J.L., Gajiwala, K.S., Maffei, M., Cohen, S.L., Chait, B.T., Rabinowitz, D., et al., 1995. Weight-reducing effects of the plasma protein encoded by the obese gene. Science 269(5223):543–546.

 

[14] Scherer, P.E., Williams, S., Fogliano, M., Baldini, G., Lodish, H.F., 1995. A novel serum protein similar to C1q, produced exclusively in adipocytes. Journal of Biological Chemistry 270(45):26746–26749.
[15] Bluher, M., Mantzoros, C.S., 2015. From leptin to other adipokines in health and disease: facts and expectations at the beginning of the 21st century. Metabolismo 64(1):131–145.
[16] Matsuzawa, Y., 2010. Establishment of a concept of visceral fat syndrome and discovery of adiponectin. Proceedings of the Japan Academy Series B Physical and Biological Sciences 86(2):131–141.
[17] Qatanani, M., Lazar, M.A., 2007. Mechanisms of obesity-associated insulin resistance: many choices on the menu. Genes & Development 21(12):1443–1455.
[18] Nedergaard, J., Cannon, B., 2014. The browning of white adipose tissue: some burning issues. Cell Metabolism 20(3):396–407.
[19] Richardson, D.K., Czech, M.P., 1978. Primary role of decreased fatty acid synthesis in insulin resistance of large rat adipocytes. American Journal of Physiology 234(2):E182–E189.
[20] Richardson, D.K., Czech, M.P., 1979. Diminished activities of fatty acid synthesis enzymes in insulin-resistant adipocytes from spontaneously obese rats. Hormone and Metabolic Research 11(7):427–431.
[21] Czech, M.P., 1976. Cellular basis of insulin insensitivity in large rat adipocytes. Journal of Clinical Investigation 57(6):1523–1532.
[22] Diraison, F., Dusserre, E., Vidal, H., Sothier, M., Beylot, M., 2002. Increased hepatic lipogenesis but decreased expression of lipogenic gene in adipose tissue in human obesity. American Journal of Physiology. Endocrinology and Metabolism 282(1):E46–E51.
[23] Roberts, R., Hodson, L., Dennis, A.L., Neville, M.J., Humphreys, S.M., Harnden, K.E., et al., 2009. Markers of de novo lipogenesis in adipose tissue: associations with small adipocytes and insulin sensitivity in humans. Diabetologia 52(5):882–890.
[24] Diraison, F., Yankah, V., Letexier, D., Dusserre, E., Jones, P., Beylot, M., 2003. Differences in the regulation of adipose tissue and liver lipogenesis by carbohydrates in humans. The Journal of Lipid Res 44(4):846–853.
[25] Guo, Z.K., Cella, L.K., Baum, C., Ravussin, E., Schoeller, D.A., 2000. De novo lipogenesis in adipose tissue of lean and obese women: application of deuterated water and isotope ratio mass spectrometry. International Journal of Obesity and Related Metabolic Disorders 24(7):932–937.
[26] Strawford, A., Antelo, F., Christiansen, M., Hellerstein, M.K., 2004. Adipose tissue triglyceride turnover, de novo lipogenesis, and cell proliferation in humans measured with $2H_2O$. American Journal of Physiology. Endocrinology and Metabolism 286(4):E577–E588.
[27] Yilmaz, M., Claiborn, K.C., Hotamisligil, G.S., 2016. De novo lipogenesis products and endogenous Lipokines. Diabetes 65(7):1800–1807.
[28] Smith, U., Kahn, B.B., 2016. Adipose tissue regulates insulin sensitivity: role of adipogenesis, de novo lipogenesis and novel lipids. Journal of Internal Medicine 280(5):465–475.
[29] Cao, H., Gerhold, K., Mayers, J.R., Wiest, M.M., Watkins, S.M., Hotamisligil, G.S., 2008. Identification of a lipokine, a lipid hormone linking adipose tissue to systemic metabolism. Cell 134(6):933–944.
[30] Yore, M.M., Syed, I., Moraes-Vieira, P.M., Zhang, T., Herman, M.A., Homan, E.A., et al., 2014. Discovery of a class of endogenous mammalian lipids with anti-diabetic and anti-inflammatory effects. Cell 159(2):318–332.
[31] Lodhi, I.J., Yin, L., Jensen-Urstad, A.P., Funai, K., Coleman, T., Baird, J.H., et al., 2012. Inhibiting adipose tissue lipogenesis reprograms thermogenesis and PPARgamma activation to decrease diet-induced obesity. Cell Metabolism 16(2):189–201.
[32] Solinas, G., Boren, J., Dulloo, A.G., 2015. De novo lipogenesis in metabolic homeostasis: more friend than foe? Molecular Metabolism 4(5):367–377.
[33] Zhao, S., Torres, A., Henry, R.A., Trefely, S., Wallace, M., Lee, J.V., et al., 2016. ATP-citrate lyase controls a glucose-to-Acetate metabolic switch. Cell Reports 17(4):1037–1052.
[34] Carrer, A., Parris, J.L., Trefely, S., Henry, R.A., Montgomery, D.C., Torres, A., et al., 2017. Impact of a high-fat diet on tissue Acyl-CoA and histone acetylation levels. Journal of Biological Chemistry 292(8):3312–3322.
[35] Wei, X., Schneider, J.G., Shenouda, S.M., Lee, A., Towler, D.A., Chakravarthy, M.V., et al., 2011. De novo lipogenesis maintains vascular homeostasis through endothelial nitric-oxide synthase (eNOS) palmitoylation. Journal of Biological Chemistry 286(4):2933–2945.
[36] Wei, X., Yang, Z., Rey, F.E., Ridaura, V.K., Davidson, N.O., Gordon, J.I., et al., 2012. Fatty acid synthase modulates intestinal barrier function through palmitoylation of mucin 2. Cell Host & Microbe 11(2):140–152.
[37] Herman, M.A., Peroni, O.D., Villoria, J., Schön, M.R., Abumrad, N.A., Blüher, M., et al., 2012. A novel ChREBP isoform in adipose tissue regulates systemic glucose metabolism. Nature 484(7394):333–338.
[38] Carvalho, E., Kotani, K., Peroni, O.D., Kahn, B.B., 2005. Adipose-specific overexpression of GLUT4 reverses insulin resistance and diabetes in mice lacking GLUT4 selectively in muscle. American Journal of Physiology. Endocrinology and Metabolism 289(4):E551–E561.
[39] Kim, J.K., 2009. Hyperinsulinemic-euglycemic clamp to assess insulin sensitivity in vivo. Methods in Molecular Biology 560:221–238.
[40] Pedersen, D.J., Guilherme, A., Danai, L.V., Heyda, L., Matevossian, A., Cohen, J., et al., 2015. A major role of insulin in promoting obesity-associated adipose tissue inflammation. Molecular Metabolism 4(7):507–518.
[41] Danai, L.V., Flach, R.J., Virbasius, J.V., Menendez, L.G., Jung, D.Y., Kim, J.H., et al., 2015. Inducible deletion of protein kinase Map4k4 in obese mice improves insulin sensitivity in liver and adipose tissues. Molecular and Cellular Biology 35(13):2356–2365.
[42] Livak, K.J., Schmittgen, T.D., 2001. Analysis of relative gene expression data using real-time quantitative PCR and the 2(-Delta Delta C(T)) Method. Methods 25(4):402–408.
[43] Schmittgen, T.D., Livak, K.J., 2008. Analyzing real-time PCR data by the comparative C(T) method. Nature Protocols 3(6):1101–1108.
[44] Aune, U.L., Ruiz, L., Kajimura, S., 2013. Isolation and differentiation of stromal vascular cells to beige/brite cells. Journal of Visualized Experiments(73).
[45] Seale, P., Conroe, H.M., Estall, J., Kajimura, S., Frontini, A., Ishibashi, J., et al., 2011. Prdm16 determines the thermogenic program of subcutaneous white adipose tissue in mice. Journal of Clinical Investigations 121(1):96–105.
[46] Wu, M., Singh, S.B., Wang, J., Chung, C.C., Salituro, G., Karanam, B.V., et al., 2011. Antidiabetic and antisteatotic effects of the selective fatty acid synthase (FAS) inhibitor platensimycin in mouse models of diabetes. Proceedings of the National Academy of Sciences of the United States of America 108(13):5378–5383.
[47] Singh, S.B., Kang, L., Nawrocki, A.R., Zhou, D., Wu, M., Previs, S., et al., 2016. The fatty acid synthase inhibitor platensimycin improves insulin resistance without inducing liver steatosis in mice and monkeys. PLoS One 11(10):e0164133.
[48] Turner, N., Kowalski, G.M., Leslie, S.J., Risis, S., Yang, C., Lee-Young, R.S., et al., 2013. Distinct patterns of tissue-specific lipid accumulation during the induction of insulin resistance in mice by high-fat feeding. Diabetologia 56(7):1638–1648.
[49] Jeffery, E., Berry, R., Church, C.D., Yu, S., Shook, B.A., Horsley, V., et al., 2014. Characterization of Cre recombinase models for the study of adipose tissue. Adipocyte 3(3):206–211.
[50] Fu, J., Li, Z., Zhang, H., Mao, Y., Wang, A., Wang, X., et al., 2015. Molecular pathways regulating the formation of brown-like adipocytes in white adipose tissue. Diabetes Metabolism Research and Reviews 31(5):433–452.
[51] Bartness, T.J., Ryu, V., 2015. Neural control of white, beige and brown adipocytes. International Journal of Obesity Supplements 5(Suppl 1):S35–S39.
[52] Yang, X., Ruan, H.B., 2015. Neuronal control of adaptive thermogenesis. Frontiers in Endocrinology (Lausanne) 6:149.
[53] Vitali, A., Murano, I., Zingaretti, M.C., Frontini, A., Ricquier, D., Cinti, S., 2012. The adipose organ of obesity-prone C57BL/6J mice is composed of mixed white and brown adipocytes. The Journal of Lipid Research 53(4):619–629.

 

[54] Schulz, T.J., Huang, P., Huang, T.L., Xue, R., McDougall, L.E., Townsend, K.L., et al., 2013. Brown-fat paucity due to impaired BMP signalling induces compensatory browning of white fat. Nature 495(7441):379–383.

[55] Tang, H.N., Tang, C.Y., Man, X.F., Tan, S.W., Guo, Y., Tang, J., et al., 2017. Plasticity of adipose tissue in response to fasting and refeeding in male mice. Nutrition and Metabolism (London) 14:3.

[56] Kursawe, R., Caprio, S., Giannini, C., Narayan, D., Lin, A., D'Adamo, E., et al., 2013. Decreased transcription of ChREBP-alpha/beta isoforms in abdominal subcutaneous adipose tissue of obese adolescents with prediabetes or early type 2 diabetes: associations with insulin resistance and hyperglycemia. Diabetes 62(3):837–844.

[57] Eissing, L., Scherer, T., Tödter, K., Knippschild, U., Greve, J.W., Buurman, W.A., et al., 2013. De novo lipogenesis in human fat and liver is linked to ChREBP-beta and metabolic health. Nature Communications 4:1528.

[58] Cannon, B., Nedergaard, J., 2004. Brown adipose tissue: function and physiological significance. Physiological Reviews 84(1):277–359.

[59] Scherer, T., O'Hare, J., Diggs-Andrews, K., Schweiger, M., Cheng, B., Lindtner, C., et al., 2011. Brain insulin controls adipose tissue lipolysis and lipogenesis. Cell Metabolism 13(2):183–194.

[60] Zhu, Y., Gao, Y., Tao, C., Shao, M., Zhao, S., Huang, W., et al., 2016. Connexin 43 mediates white adipose tissue beiging by facilitating the propagation of sympathetic neuronal signals. Cell Metabolism 24(3):420–433.

[61] Garretson, J.T., Szymanski, L.A., Schwartz, G.J., Xue, B., Ryu, V., Bartness, T.J., 2016. Lipolysis sensation by white fat afferent nerves triggers brown fat thermogenesis. Molecular Metabolism 5(8):626–634.

[62] Parimisetty, A., Dorsemans, A.C., Awada, R., Ravanan, P., Diotel, N., Lefebvre d'Hellencourt, C., 2016. Secret talk between adipose tissue and central nervous system via secreted factors-an emerging frontier in the neurodegenerative research. Journal of Neuroinflammation 13(1):67.

[63] Xiong, X.Q., Chen, W.W., Zhu, G.Q., 2014. Adipose afferent reflex: sympathetic activation and obesity hypertension. Acta Physiologica (Oxford) 210(3):468–478.

[64] de Lartigue, G., Ronveaux, C.C., Raybould, H.E., 2014. Deletion of leptin signaling in vagal afferent neurons results in hyperphagia and obesity. Molecular Metabolism 3(6):595–607.

[65] Niijima, A., 1999. Reflex effects from leptin sensors in the white adipose tissue of the epididymis to the efferent activity of the sympathetic and vagus nerve in the rat. Neuroscience Letters 262(2):125–128.

[66] Bartelt, A., Weigelt, C., Cherradi, M.L., Niemeier, A., Tödter, K., Heeren, J., et al., 2013. Effects of adipocyte lipoprotein lipase on de novo lipogenesis and white adipose tissue browning. Biochimica et Biophysica Acta 1831(5): 934–942.

[67] Ye, R., Wang, Q.A., Tao, C., Vishvanath, L., Shao, M., McDonald, J.G., et al., 2015. Impact of tamoxifen on adipocyte lineage tracing: inducer of adipogenesis and prolonged nuclear translocation of Cre recombinase. Molecular Metabolism 4(11):771–778.

[68] Czech, M.P., 2017. Insulin action and resistance in obesity and type 2 diabetes. Nature Medicine in press.

 